5874–5886 *Nucleic Acids Research, 2013, Vol. 41, No. 11* *Published online 22 April 2013*
doi:10.1093/nar/gkt271

An aromatic residue switch in enhancer-dependent bacterial RNA polymerase controls transcription intermediate complex activity

Simone C. Wiesler[1,*], Robert O. J. Weinzierl[2] and Martin Buck[1,*]

[1]Division of Cell and Molecular Biology, Department of Life Sciences, Imperial College London, London, SW7 2AZ, UK and [2]Division of Molecular Biosciences, Department of Life Sciences, Imperial College London, London, SW7 2AZ, UK

Received January 15, 2013; Revised and Accepted March 25, 2013

ABSTRACT

The formation of the open promoter complex (RPo) in which the melted DNA containing the transcription start site is located at the RNA polymerase (RNAP) catalytic centre is an obligatory step in the transcription of DNA into RNA catalyzed by RNAP. In the RPo, an extensive network of interactions is established between DNA, RNAP and the σ-factor and the formation of functional RPo occurs via a series of transcriptional intermediates (collectively 'RPi'). A single tryptophan is ideally positioned to directly engage with the flipped out base of the non-template strand at the +1 site. Evidence suggests that this tryptophan (i) is involved in either forward translocation or DNA scrunching and (ii) in σ^{54}-regulated promoters limits the transcription activity of at least one intermediate complex (RPi) before the formation of a fully functional RPo. Limiting RPi activity may be important in preventing the premature synthesis of abortive transcripts, suggesting its involvement in a general mechanism driving the RPi to RPo transition for transcription initiation.

INTRODUCTION

Gene expression is controlled and regulated at many stages, e.g. epigenetically, transcriptionally, translationally and through post-translational modifications. Transcription initiation is particularly amenable to regulation owing to the large number of binding or catalytic reactions occurring and owing to the complexity of the molecular interfaces existing between the many factors involved. Fundamentally, the mechanics and chemistry of transcription are conserved across the three domains of life and are set by key functional properties of the RNA polymerases (RNAPs) and their associated transcription factors (1,2). However, some functions of the transcription apparatus are organism specific. For example, understanding the precise details of the transcription mechanism of a species and how they differ from those of others opens up options for targeted drug development against pathogens or formulation of pathway specific inhibitors (3).

Bacterial transcription is essentially regulated by two classes of sigma (σ) factors, σ^{70} whose eponymous member controls the transcription of housekeeping genes, and σ^{54} for the expression of genes whose products counteract stress situations (4–7). Both classes of σ-factors bind core RNAPs (E) to form holoenzymes (Eσ) that then bind to specific classes of promoters and initially form closed promoter complexes (RPcs) with a fully duplexed DNA template. Subsequently, transition into a transcriptionally competent open promoter complex (RPo) occurs. $E\sigma^{70}$ holoenzymes undergo the required conformational changes spontaneously. $E\sigma^{54}$, on the other hand, relies on the action of a bacterial enhancer binding protein (bEBP). These bEBPs use adenosine triphosphate (ATP) hydrolysis to remodel RPc for the formation of melted DNA in the RNAP active centre where the start site is available in single-stranded form and templated RNA synthesis can occur (4,6,8–12). A pathway to RPo formation from the RPc has been proposed in which a bEBP-bound $E\sigma^{54}$ complex, called RPi, is formed in which ATP hydrolysis is yet to occur (13).

Multiple interactions are established between the RNAP and the σ-factor, the σ-factor and the DNA template/non-template strands and the RNAP and the DNA template/non-template strands (14–16). These interactions precisely position the +1 start site DNA in the active centre, and their making and breaking accommodate the structural rearrangements, such as melting of the

*To whom correspondence should be addressed. Tel: +44 207 594 5366; Fax: +44 207 594 5419; Email: s.wiesler@imperial.ac.uk
Correspondence may also be addressed to Martin Buck. Tel: +44 207 594 5442; Fax: +44 207 594 5419; Email: m.buck@imperial.ac.uk

DNA template and RNAP clamp closure. The clamp is formed by the β′ subunit, and by closing over the active centre cleft it holds RNA and DNA in place during transcription (17,18). To achieve this, these interactions need to be dynamic and highly coordinated.

We have previously described the contribution of the RNAP switch regions to the opening of the transcription start site by demonstrating that transcriptional defects caused by point mutations in the switch regions can be rescued by pre-opening the +1 site (19). A recent structural study suggests that the non-template strand +1 site is contacted by residue βW183 of the β subunit of *Escherichia coli* RNAP (Figure 1C). According to this model, which is derived from a σ^{70}-dependent RNAP and promoter, the +2 G of the non-template strand fits into a pocket formed by the β subunit of RNAP and subsequently β W183 undergoes stacking interactions with the +1T. This arrangement is in agreement with previously reported cross-linking data (14,16).

We considered that the start site opening mechanism for σ^{54} regulated transcription that is controlled by the switch regions might ultimately converge on βW183 in *E.coli* RNAP. Through strong stacking interactions with the +1 site, the βW183 residue could act to pull or capture the non-template strand away from the template strand potentially making its +1 site accessible to the incoming nucleotide. However, no biochemically detectable phenotype has been reported for an alanine substitution mutant of βW183 (16). The difficulties to detect a phenotype with βW183A may reflect a caveat of σ^{70}-regulated transcription where the RPi states are short-lived and transient and therefore barely accessible to biochemical investigations. The σ^{54}-regulated system, on the other hand, with its requirement for ATP hydrolysis to progress from the RPi to the RPo, allows us to trap the Eσ^{54}-bEBP complex at a point just before ATP hydrolysis, which is believed to represent one state of the RPi. Hence, the σ^{54}-regulated system may be much better suited to identify phenotypes that affect the RPi than is the σ^{70}-regulated system.

We anticipate that some similar interactions to those reported for σ^{70} are established in a σ^{54}-dependent system, and, here, we provide evidence that for enhancer-dependent transcription βW183 keeps the transcribing activity of an intermediate complex (RPi) in check to prevent transcription from occurring prematurely during the RPc to RPi and to RPo interconversions. Finally, we propose that βW183 may have an additional role in mediating template forward translocation or DNA scrunching during transcription elongation.

MATERIALS AND METHODS

Mutagenesis

Single amino acid substitutions of the *E. coli rpoB* gene (pIA545) were introduced by site-directed mutagenesis and reconstituted in pVS10 as previously described (19,20).

DNA probes and proteins

DNA templates representing the *Sinorhizobium meliloti nifH* or the lacUV5 promoter were 5′-^{32}P-labelled (where appropriate) and annealed to the complementary strand as described (22). Sequences of the promoter constructs are listed in Supplementary Table S1. *Escherichia coli* RNAP [wild-type (WT) and βW183 variants], $PspF_{1–275}$ and *Klebsiella pneumoniae* σ^{54} were overexpressed in *E. coli* and purified as described (9,23,24). *Escherichia coli* σ^{70} was a gift from S. Wigneshweraraj, PspF D108A was a gift from N. Joly and PspF F85A was a gift from N. Zhang.

Eσ^{54} formation assays

A total of 1 μM ^{32}P-HMK- σ^{54} (gift from N. Joly) were incubated with 25–100 nM RNAP (WT or switch variants) and 500 μg/ml α-lactalbumin in standard Tris-acetate (STA) buffer [25 mM tris-acetate (pH 8.0), 8 mM magnesium acetate, 10 mM KCl, 3.5% (w/v) PEG6000] at 37°C for 15 min. The reactions were quenched by adding native buffer, and the Eσ^{54} holoenzyme complexes formed were analysed on 4.5% non-denaturing gels. Products were visualized and quantified using a Fuji FLA-5000 PhosphorImager. For quantitation purposes, the PSL transfer scale was adjusted using the AIDA software, and for illustration purposes, the Curves scale was adjusted using Photoshop CS3. All Eσ^{54} formation assays were performed as titrations at three different RNAP concentrations (25 nM, 50 nM, 100 nM). The titrations were conducted to ensure that the observed effects were not distorted due to assay saturation effects. For each RNAP concentration, the activity was calculated relative to WT activity (in %). This provided us with triplicate results for the relative activities of each variant, which were then averaged, and standard deviations were calculated.

Minimal scaffold assays

Specific promoter-independent transcription assays ('minimal scaffold assays') were performed as described (24) using 100 nM of a minimal scaffold template that was constructed by first annealing the DNA strands 5-G GTCCTGTCTGAAATTGTTATCCGCTAC (template) and 5-ACAATTTCAGACAGGACC (non-template) to which a priming RNA molecule of either seven bases (5-GUAGCGG) or eight bases (5-GUAGCGGA) in length was annealed. These assays permit determination of the catalytic activity of the RNAP variants in the absence of any requirements for promoter recognition or interaction with σ factors. The reactions were carried out in STA buffer. RNA synthesis was initiated by addition of 25, 50 and 100 nM core RNAP (WT or W183 variants) and 1 μCi of α^{32}P-UTP. The reactions were incubated at 37°C for 15 min, quenched by addition of loading buffer and analysed on 20% denaturing gels as described earlier in the text.

Inorganic pyrophosphate assay

In the post-extension state, RNAPs are capable of catalysing the cleavage of the terminal nucleotide from a transcript on addition of inorganic pyrophosphate (PPi). This activity is pyrophosphorolysis and is one of the proofreading mechanisms of RNAP (25).

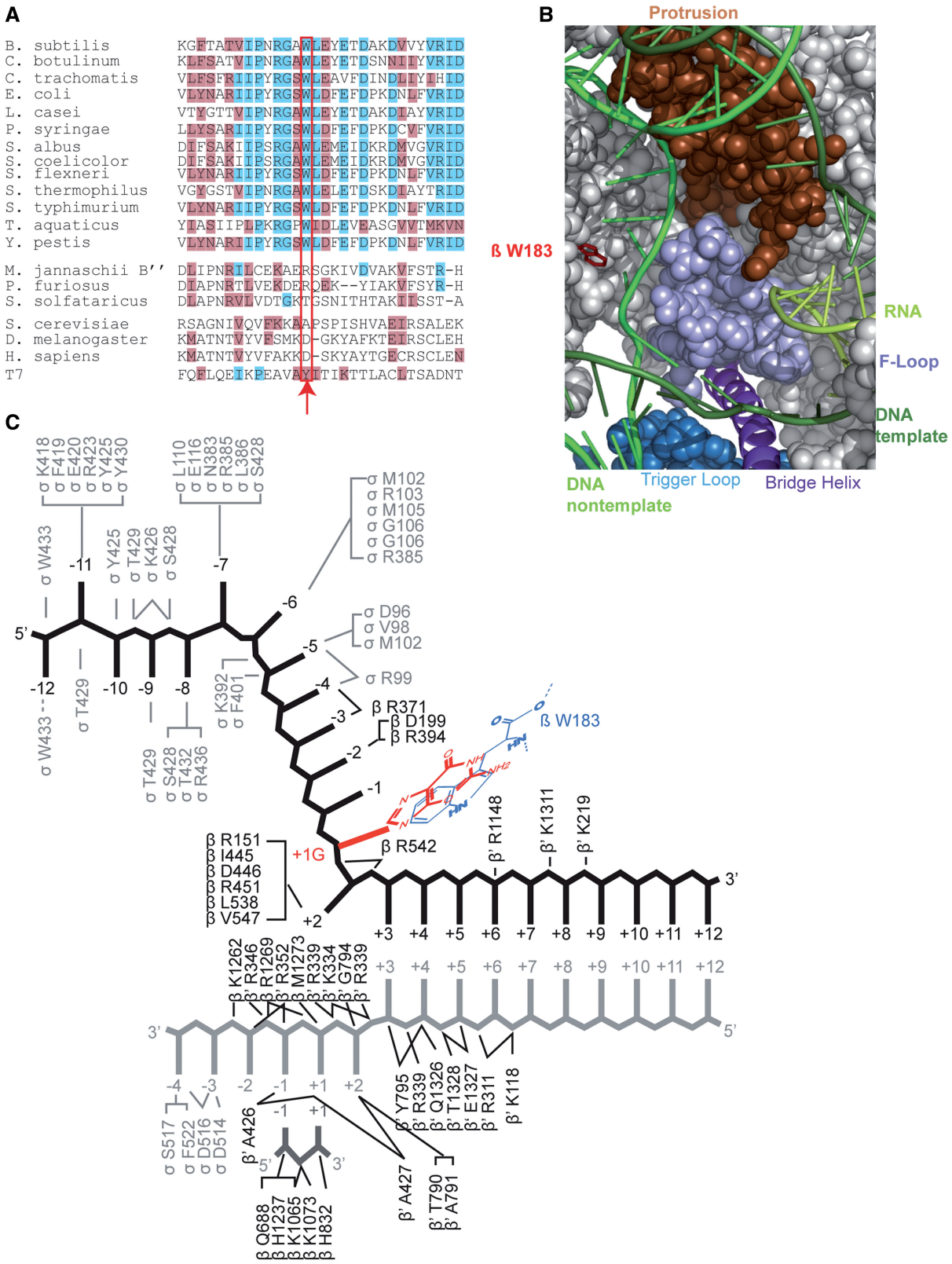

Figure 1. βW183 is highly conserved in bacteria and acts in a complex network in the active centre. (**A**) ClustalW analysis of bacterial, archaeal and eukaryotic species illustrate a strong conservation of βW183 in bacteria, with no counterpart in the corresponding archaeal or eukaryotic RNAP subunits. (**B**) In a model of the TEC βW183 is in close proximity to the non-template strand near the active centre (21). (**C**) βW183 engages in a complex network between the RNAP, the σ-factor and the nucleic acids in the active centre and interacts with the non-template +1 site [adapted from (16)].

Pyrophosphatase assays were performed as described (20) by using 100 nM of the minimal scaffold assembly containing the α^{32}P-labelled 7 nt RNA in the presence of 0.5 mM pyrophosphate. Reactions were initiated on addition of 25 nM, 50 nM or 100 nM core RNAP, incubated at 37°C for 10 min and analysed on 20% denaturing gels.

Binding assays

Minimal scaffold and promoter binding assays were conducted as described (24,26,27). Native gel mobility shift assays, both on the minimal scaffold and on *nifH* promoter probes, were conducted in STA buffer in a total reaction volume of 10 µl containing 25, 50 and 100 nM core RNAP or Eσ^{54} (reconstituted with σ^{54} as described earlier in the text) and 25 nM α^{32}P-labelled probe, which was incubated for 15 min at 37°C. RPos and RPi were formed as described earlier in the text. The reactions were analysed using a 4.5% native gel run at 100 V for 55 min. The gels were dried and protein–DNA complexes were analysed as described earlier in the text.

Small-primed RNA assays

Promoter-dependent small-primed RNA (spRNA) assays (a form of abortive initiation assay in which only a subset of ribonucleotide triphosphates [rNTPs] are present) were performed as described (26) in STA buffer, in a 10-µl reaction volume containing 25–100 nM Eσ^{54} (reconstituted using 40 µM of σ and 25, 50 and 100 nM RNAP) and 0.5 mM dATP. ADP•AlF trapped complexes for RPi formation were formed as described (26) in STA buffer, in a 10-µl reaction volume containing 25–100 nM Eσ^{54} (reconstituted using 40 µM of σ and 25–100 nM RNAP), 2 mM dADP and 2.5 mM NaF. The samples were initially incubated at 37°C for 15 min to form Eσ^{54} complexes. Then, 25 nM double-stranded variations of the *Sinorhizobium meliloti nifH* promoter were added for 10 min at 37°C. Open complex formation was initiated by adding 7 µM $PspF_{1\text{-}275}$ for 10 min at 37°C. For trapped complexes (to make RPi), 0.2 mM AlCl3 was added for 10 min at 37°C. Finally, synthesis of spRNA (UpGGG) was initiated by adding an elongation mix containing 200 µg/ml heparin, 0.5 mM UpG and 1 µCi α^{32}P-guanosine triphosphate (GTP). The reactions were incubated at 37°C for 20 min and quenched by addition of loading buffer. Portions of the samples were analysed on a 20% denaturing gel and visualized and quantified as described earlier in the text.

RNA retention assay

The spRNA assays were carried out as described earlier in the text, but the sample was split after the elongation step. One portion each was mixed with native or formamide loading dye for analysis under native or denaturing conditions, respectively.

Molecular dynamics

The transcription elongation complex (TEC) model structure was analysed by fully atomistic conventional molecular dynamics and by an enhanced sampling method [accelerated MD (aMD); (28)] using the AMBER12 simulation package. The fully parameterized and charge-neutralized model was initially equilibrated at 300 Kelvin in a TIP3P water octahedral waterbox at constant pressure and subjected to 7.5 nanoseconds (ns) of graphics processing unit (GPU)-supported conventional molecular dynamic (isothermal–isobaric [constant Number, Pressure, Temperature] ensemble) in Single Precision Double Precision hybrid calculation mixed precision mode (29). To explore conformational changes occurring for a longer period, aMD was performed with extra boosts to dihedral and whole potential energies, resulting in an enhancement of simulation efficiency by a factor of ~2000 (28). The diehedral and total energy boosts were calculated as described (28) based on the energy values observed after the initial 7.5 ns.

The resulting trajectories were analysed and visualized using Visual Molecular Dynamics (30).

RESULTS

βW183 is highly conserved in bacteria, but not in archaeal or eukaryotic species

Cross-linking and structural data using *Thermus thermophilus* RNAP and σ^{70} strongly suggest βW183 interacts with the +1 site on the non-template strand during transcription initiation (14,16). Sequence alignments of bacterial RNAP β subunits with archaeal B or B″ and eukaryotic Rpb2 sequences highlight a strict conservation of this residue across all bacterial species examined (Figure 1A). However, no orthologs of βW183 were found in either the archaeal or the eukaryotic RNAP subunits. As σ-factors are unique to bacteria, the presence of this residue in bacteria without an obvious counterpart in the archaea or eukaryotes may reflect a mechanism that involves all or a subset of σ-factors at promoters. Structural analyses illustrate that β W183 is within close proximity of the non-template strand at a distance of ~40 Å from Metal A of the catalytic site, suggesting that its influence on the actual catalytic reaction is limited or non-existent. βW183 may engage with the non-template +1 site indicating a potential role in start site opening (Figure 1A and B). These structural data were used and extrapolated to explain the findings in our Eσ^{54}-dependent systems, which are illustrated below (Figure 1C).

βW183 variants are catalytically active but defective in binding minimal scaffolds and holoenzyme formation

Single residue substitutions were created at position βW183 to investigate the residue's effect on various steps in the transcription initiation process using the *E. coli* RNAP. An alanine substitution was created to remove the aromatic while preserving mild hydrophobic properties, a serine substitution introduced hydrophilic properties and aspartate and arginine substitutions introduced negative or positively charged sidechains, respectively. We tested these mutants in a number of *in vitro* assays to assess their catalytic activity and their capacity to bind DNA and to form holoenzymes (Figure 2).

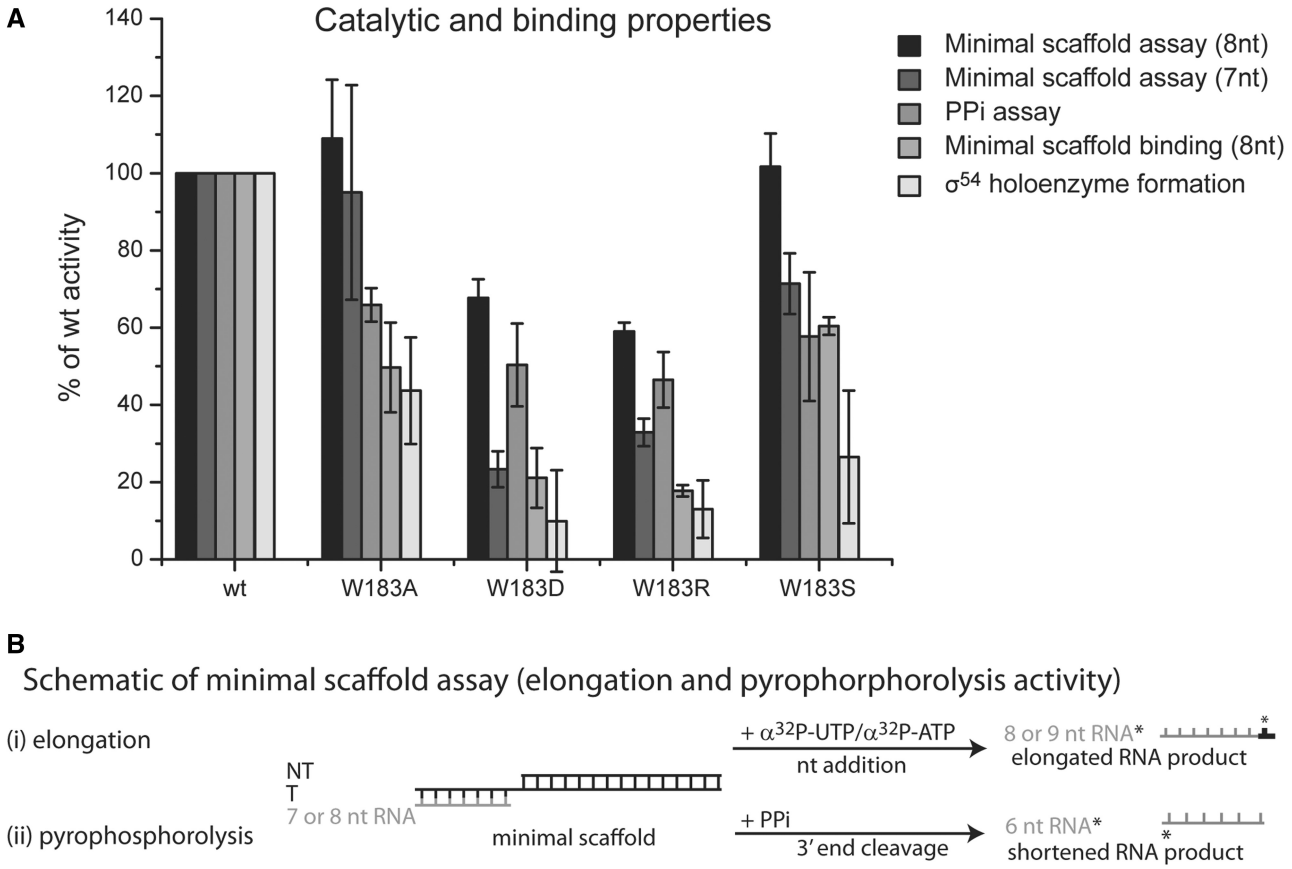

Figure 2. Catalytic and binding properties (**A**) βW183 mutants are defective in nucleic acid binding and holoenzyme formation in comparison with wild-type RNAP (wt). The catalytic defects of the variants can in part be explained by the defects in scaffold binding and holoenzyme formation. The assays were performed as titrations at three different RNAP concentrations (25 nM, 50 nM, 100 nM). The activity for each mutant was calculated relative to the WT activity. The data represent average activities, and the error bars represent standard deviations. For each reaction, 33 nM of α^{32}P-GTP was used. The GTP turnover into RNA achieved by the WT in a minimal scaffold assay (7 nt RNA) was 6 nM (25 nM RNAP), 9 nM (50 nM RNAP) or 17 nM (100 nM RNAP), respectively. (**B**) Schematic of the minimal scaffold assay measuring RNA elongation (minimal scaffold assay) and pyrophosphorolysis (PPi assay) activities. For minimal scaffold binding assays, the minimal scaffold was ^{32}P-labelled, incubated with RNAP and complexes were separated on a native gel.

In minimal nucleic acid scaffold-directed transcription assays, an RNA primer was hybridized to a DNA scaffold and extended by a single radiolabelled nucleotide. βW183A and βW183S performed WT-like in these assays, whereas the activity of βW183D and βW183R was reduced to 20–70%. These observations are consistent with those of others (16) and also with pyrophosphate catalyzed RNA cleavage assays where the terminal nucleotide of the RNA primer is cleaved on addition of PPi (Figure 2). The RNA extension and cleavage activities in βW183 variants establish that βW183 is largely dispensable for the catalytic function of RNAP. Stronger defect phenotypes were observed in nucleic acid binding and also in Eσ^{54} formation assays where all four mutants showed only between 10 and 65% of WT activity (Figure 2). Again, the defects of βW183D and βW183R were more pronounced. The nucleic acid-binding defects can account for the apparent reduction in catalytic activity, suggesting that the mutants are fully catalytically active. The defects in scaffold and σ-factor binding likely reflect changes in the complex network of interactions between the scaffold, the RNAP and the σ-factor that βW183 has been postulated to participate in (16).

The failure to properly engage with nucleic acids and σ^{54} is directly reflected in the mutants' modestly compromised ability to form RPcs that reached 60–95% of WT levels (Figure 3). With Eσ^{54}, it is possible to stably form an intermediate complex by the binding of its cognate activator to RPc to form RPi. The RPi can be trapped by adding the nucleotide analogue ADP-AlF, which mimics the conformation of the nucleotide just prior to ATP hydrolysis (26). Formation of the RPi with Eσ^{54} by adding PspF and ADP-AlF to the RPcs were not affected, and for all RNAP variants comparable fractions (40–45%) of the RPc shifted into the RPi (Figure 3). When allowing the activator-driven ATP hydrolysis reaction to proceed and RPos to form, the defects became more pronounced with the mutants forming 20–60% RPos in comparison to WT (Figure 3). This suggested that, in addition to their defects in binding DNA and σ^{54}, the mutants are also impaired in their capacity to form RPos with the two effects being additive. A 50% reduction in the amount of mutant as compared with

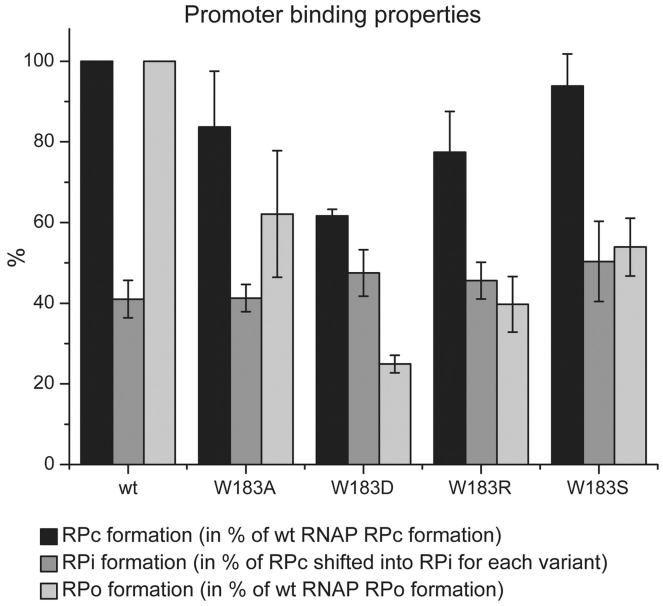

Figure 3. Promoter-binding properties. βW183 mutants are mildly defective in RPc formation, which can be explained by their general defects in holoenzyme formation and DNA binding. Although RPi formation is not affected, the mutants display additive defects in RPo formation. For RPc and RPo, the bars reflect the amount of complex that was formed relative to WT. For RPi, the bars reflect the fraction of RPc that has been converted to RPi for each variant (also see Supplementary Figure S1).

WT RPos was demonstrated by forming RPos, followed by adding heparin as a competitor and the removal of samples at regular time intervals to estimate remaining RPo levels. The stability of the complexes formed towards heparin did not seem to be affected by the mutations (Supplementary Figure S1A, right). The presence of the initiating dinucleotide UpG did not significantly stabilize the RPos, thus ruling out the possibility that the defects in RPo stability occur at the level of base pairing to the template strand (Supplementary Figure S1A, left).

RPc formation for $E\sigma^{70}$ has been reported to be more efficient on certain truncated promoter probes reflecting the energetic costs of making interactions with the downstream fork junction structure formed around +1 (31) (Supplementary Figure S1B, bottom). A similar effect was not observed with $E\sigma^{54}$, and its cognate nifH promoter probes truncated at −5/−5, +2/+2 and +6/+6, presumably reflecting the lack of any extensive downstream fork junction formation in the $E\sigma^{54}$ RPcs. Formation of −5/−5 RPcs was comparable with RPc formation on WT/WT templates, whereas +2/+2 and +6/+6 templates formed only a third of the number of RPcs. This suggests that some energetically favourable interactions before RPo formation are made by $E\sigma^{54}$ with sequences downstream of +1. RPc formation on all four templates was at least three times lower than on a (−10−1)/WT template, which contained a mismatch between the non-template and template strands from the −10 to the −1 site, mimicking a transcription bubble (Supplementary Table S1). Also, the signals obtained on templates other than the (−10−1)/WT template were weak. Although the mutants apparently recovered their ability to form RPcs on these templates in comparison with WT, the overall weak signal intensity does not permit unambiguous quantitative conclusions about such a recovery effect (Supplementary Figure S1B, top). Nevertheless, it appears that promoter DNA sequences downstream of the start site do impact on the observable phenotypes of βW183 variants in promoter binding assays. These experiments also demonstrate that in the $E\sigma^{54}$-dependent transcription system, the presence of the downstream DNA is absolutely essential for the formation of functional RPos.

Start site opening does not rescue mutant activity in promoter directed transcription

We next tested $E\sigma^{54}$ promoter-directed transcription activity by carrying out spRNA transcription assays using a linearized *nifH* promoter probe with a mismatch from −10 to −1 [(−10−1)/WT], thus creating an artificial transcription bubble. After formation of RPcs and addition of the activator protein PspF and ATP, a dinucleotide RNA primer (UpG, −1+1) was extended by one or two labelled nucleotides to form an abortive trimeric or tetrameric product (26). In these assays, βW183A and βW183S performed WT-like, whereas the activity of βW183D and βW183R was reduced to ∼40% (Figure 4). These results reiterate and reinforce the promoter binding observations described earlier in the text (Figures 2 and 3). The more severe defects of the W183D and W183R mutants are probably due to the greater structural impact on the introduction of side chain charges, whereas the W183S and W183A, which maintain the neutral charge of the tryptophan cause less severe structural disruptions. To investigate whether the observed changes were due to altered affinities of the RNAP variants to GTP, we performed spRNA assays under high nucleotide concentration conditions (Supplementary Figure S3). On addition of higher concentrations of GTP, we observed a marked increase in the production of abortive transcripts. This increase was initially greater for the WT than the mutants. All five variants reached saturation at 50 μM cold GTP, but although the activity of the W183 mutants remained stable or even slightly increased at higher concentrations, the activity of the WT declined. This inhibition effect was probably due to inhibition caused by GTP competing with UpG for the start site (Supplementary Figure S2).

Because of the reported interaction of βW183 with the +1 site (16), we reasoned that a possible contribution to start site opening seemed likely. Previously, we demonstrated a role of the switch regions in start site opening by extending the artificial transcription bubble of our (−10−1)/WT template to include the +1 and +2 sites (32). Using such templates in assays with switch region point mutants led to a striking recovery from their defects in promoter-directed transcription. We concluded that the defects of these mutants are due to a failure in start site opening, which can be compensated for by bypassing +1 site opening (32).

No such recovery effect was observed with the βW183 mutants that performed in exactly the same manner as on

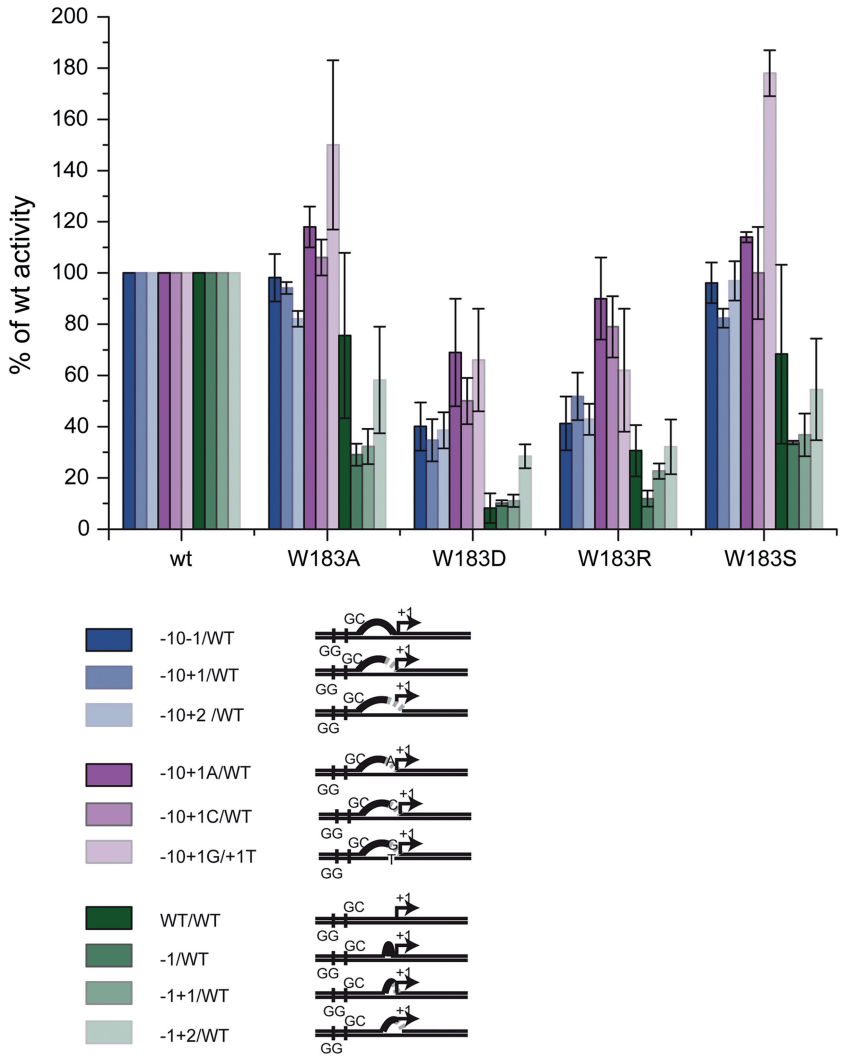

Figure 4. βW183 are WT-like or defective in promoter-directed transcription. (Top) βW183 mutants are WT-like or defective in spRNA assays testing for promoter-directed transcription. These defects are not rescued by templates with a pre-opened start site. The defects are particularly apparent with βW183D and βW183R where a charge has been introduced that presumably had a greater structural impact than the charge-neutral alanine and serine substitutions. On one of the templates (−10+1G)/+1T, these charge-neutral substitutions even slightly exceed WT activity. (Bottom) Template variants used for spRNA assays to assess the effects on start site opening.

the standard (−10−1)/WT template (Figure 4). On fully duplexed templates where only the start site and its flanking residues were melted, we observed more dramatic defects, and the mutants reached 10–75% of WT activity. This is consistent with the previously documented greater difficulties of using duplexed templates for making RPo (32) (Table 1).

The WT *nifH* promoter harbors a purine residue—G—at the non-template strand +1 site. In our templates with the pre-melted start site, we had substituted G by T to create the mismatch. To assess the requirements for a specific type of base in the +1 position, we generated additional templates with A or C in the non-template strand +1site (Figure 4). Again, we observed similar phenotypes as on the (−10−1)/WT template with βW183A and βW183S performing WT-like and βW183D and βW183R being reduced to 50–90% (Figure 4). Finally, we restored the non-template strand +1G and maintained the

Table 1. Comparison of the activity of WT RNAP on promoter templates used relative to its activity on the (−10−1)/WT template

Promoter template	Activity of WT RNAP relative to activity on (−10−1)/WT template (%)
WT/WT	5 ± 1
(−10+1)/WT	303 ± 99
(−10+2)/WT	280 ± 73
(−10+1A)/WT	363 ± 143
(−10+1C)/WT	233 ± 22
(−10+1G)/+1T	61 ± 16
(−1)/WT	64 ± 13
(−1+1)/WT	182 ± 33
(−1+2)/WT	181 ± 29

Numbers represent averages of three samples ± standard deviation.

mismatch by substituting the template +1C by T. Here, the βW183A and βW183S mutants had higher activity than the WT (150–180%), whereas the βW183D and βW183R mutants remained suppressed at 50–60% (Figure 4). These experiments argued against βW183 playing a sole role in start site opening. It is possible that the 150–180% increase with W183A and W183S and decrease to 50–60% with W183D and W183R on (−10+1G/1T) substrate is due to W183 making interactions with the incoming dinucleotide. Substitution of W183 with alanine and serine may change the RNAP's preference for binding the UpA over the UpG dinucleotide. Also, the (−10+1G)/1T template was less efficiently used (~60% efficiency in comparison with (−10−1)/WT) than all the other templates with a pre-melted template [200–400% efficiency in comparison with (−10−1)/WT] (Table 1).

We considered that the differences we observed in the performance of the mutants were due to a delayed transcript release. To investigate this possibility, we performed an RNA retention assay on both the (−10−1)/WT and the (−10+1A)/WT template: The spRNA assay was carried out as usual but after the elongation step, the reaction was split and mixed with either native buffer for separation of the reaction products on a native gel or with denaturing loading dye to analyse the total transcript on a denaturing gel. Under native conditions, we observed a high-molecular weight band representing $E\sigma^{54}$, in principle with either α^{32}P-GTP or UpGGG* bound to it. This complex was more abundant with the W183 mutants, in particular βW183A and βW183S (Supplementary Figure S3A). This was true for both templates with absolute amounts of the labelled species (i.e. bound plus released product) mirroring the efficiency with which the respective templates were used (Table 1). The proportion of the retained species was accounted for a maximum of 0.3% of the total transcript. For this reason, differences between the W183 mutants and the WT were extremely difficult to score. It was not possible to establish with certainty whether the retained species represents bound ^{32}P-GTP or UpGGG*. In conjunction with results showing that the apparent affinity of the mutants for the nucleotide is lower than that of the WT, the retained species is likely to be UpGGG*. Although the release of the RNA transcript may not in itself be a major contributing factor to the reduced performance of βW183D and βW183R (Supplementary Figure S3A), its increased retention may indicate a change in product binding.

βW183 limits the transcriptional activity of an RPi

Although RPos must be formed for optimal transcription initiation, production of short transcripts occurs from one intermediate complex, RPi, formed just before ATP hydrolysis (26). This activity is weak and presumably must be suppressed until a stable RPo is formed, which can enter the elongation phase and—by implication—productive transcription. The RPi is a transient state that is largely inaccessible for experimental investigation in $E\sigma^{70}$-mediated transcription. In contrast, the RPi created when $E\sigma^{54}$-RPc is bound by PspF can be trapped with ADP-AlF (26). Trapping can be exploited to explore the transcriptional activity of the RPi. The key position of βW183 in a structural network defining RPo is in stark contrast to its failure in producing strong mutant phenotypes in any state (RPc or RPo) that can be studied in a σ^{70}-regulated system. We therefore reasoned that βW183 may predominantly function in the RPi state. To test this hypothesis, WT and mutant $E\sigma^{54}$ complexes were trapped as RPi (Figure 5A) by adding PspF and ADP-AlF before performing spRNA reactions. Here, the βW183A and βW183S mutants displayed superactivity by reaching levels, which are up to twice as high as those reached by WT RNAP. βW183D and βW183R perform at 75% of WT activity (Figure 5B and C), a significantly higher activity than under ATP hydrolysis conditions where RPo forms (Figure 5A, B and D). These data thus provide clear evidence that βW183 functions to limit the transcribing activity of the RPi.

To test the stringency of the requirements for interactions between the non-template strand and βW183, the mismatch of the non-template strand was extended by 1, 2 or 3 bases [(−10−1)+1/WT, (−10−1)+2/WT, (−10−1)+3/WT]. We also tested a template where the non-template strand was shortened by one base [(−10−1) −1/WT) and another template where the entire −10−1 sequence of the non-template strand was deleted [Δ(−10−1)/WT] (Figure 5B). The rationale of creating these templates was to provide alternative interfaces for interactions of the non-template strand with the RNAP, thereby mimicking different stages during the structural rearrangements, such as DNA scrunching (33,34). We found an increase in mutant activity on almost all these templates, which in the case of βW183A and βW183S consistently exceeded WT activity (Figure 5B and D). The effect was weaker with βW183D and βW183R where superactivity was observed only with the (−10−1)+3/WT template (Figure 5B and D). Under trapping conditions used for forming RPi, the superactivity effect occurred to the same or an even larger extent with the mutants being up to 5-fold more active than the WT (Figure 5B and D). Similarly, we found that different forms of the RPis created by use of several PspF variants altered in their nucleotide hydrolysis and RPc binding activities also became superactive (Supplementary Figure S3B). This demonstrated that premature transcription occurs in different forms of the RPi when βW183 is absent.

βW183 may be involved in forward translocation or DNA scrunching

Simulations of the molecular dynamics (MD) of βW183 within the context of a transcription elongating complex illustrate a stable interaction of the tryptophan with the non-template strand (Figure 6A, Supplementary Movie S1). The aMD shows that this interaction can be broken, allowing βW183 to dissociate from the non-template strand (Figure 6B, Supplementary Movie S2) and in a next step engage with βR197 (Figure 6C, Supplementary Movie S3). This breaks βR197's contacts with the phosphodiester backbone and permits

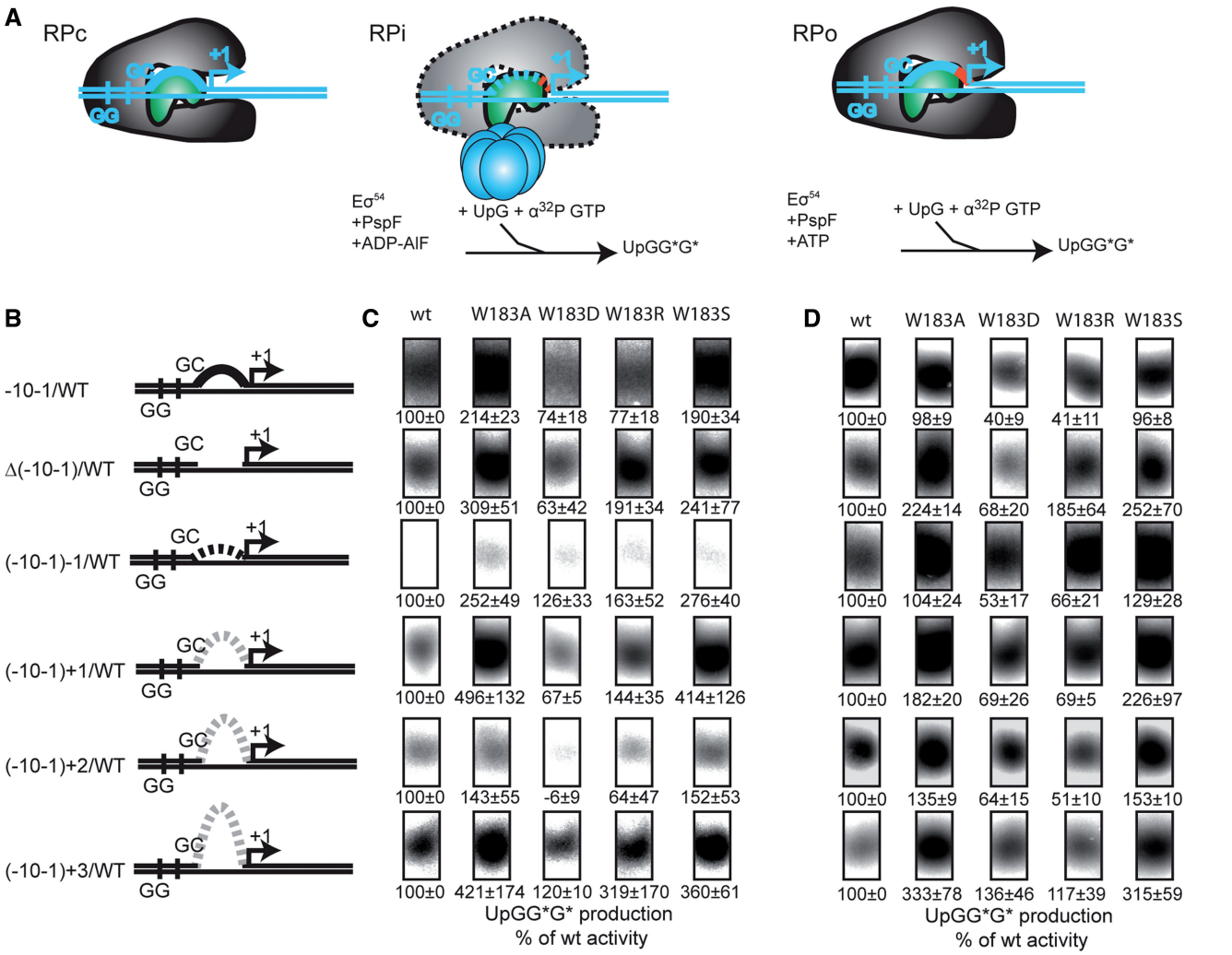

Figure 5. βW183 functions in limiting transcription activity of the RPi. (**A**) Generating labelled tetramers under trapping (RPi) and ATP hydrolysis (RPo) conditions. (**B**) Template variants used for spRNA assays to assess the effect of non-template strand length. (**C**) Under trapping conditions, the mutants are significantly more active in using templates with different non-template strand length. Assays were carried out in triplicates as titrations with 25 nM, 50 nM and 100 nM RNAP. Signal intensity was quanitified using the AIDA imaging software and normalized against the total signal per lane. Error bars represent standard deviations. (**D**) The same effect, albeit slightly weaker, is observed under ATP hydrolysis conditions (also see Supplementary Figure S3).

reengagement of βW183 and βR197 with DNA bases further downstream after translocation. The cycle of interaction, dissociation, engagement with R197 and re-engagement with the DNA is accompanied by structural rearrangements in the DNA template. The two residues thus seem to be involved in a mechanism that propels the DNA template forward and could therefore contribute to either the forward translocation mechanism of the RNAP or DNA scrunching (Supplementary Movie S1–3).

DISCUSSION

A thermodynamic sink drives RPo formation and template translocation

The nucleation of the transcription bubble, completion of the transcription bubble and RNAP clamp closure are all integral steps en route to the formation of an RPo. They are governed by conformational changes of key RNAP domains, can be orchestrated through the action of sigma factors and their promoter DNA binding interactions (15) and are therefore subject to genetic regulation. Our interest in the mechanism of start site opening in activator-dependent RPo formation had previously revealed a major and distinctive contribution of the RNAP switch regions (32). βW183, being a large aromatic residue and positioned in close proximity to the non-template +1 site, made it a likely candidate to engage in interactions with the +1 base (14,16). As such, a role in providing an interface to compete with the template strand base-pairing interactions seemed plausible; βW183 could act as a lever to open up the start site and make it accessible to incoming nucleotides. Such a scenario would tie in with a relay mechanism that is initiated by the switch regions and finally converges onto βW183. The contribution of the switch regions to start site opening had been demonstrated

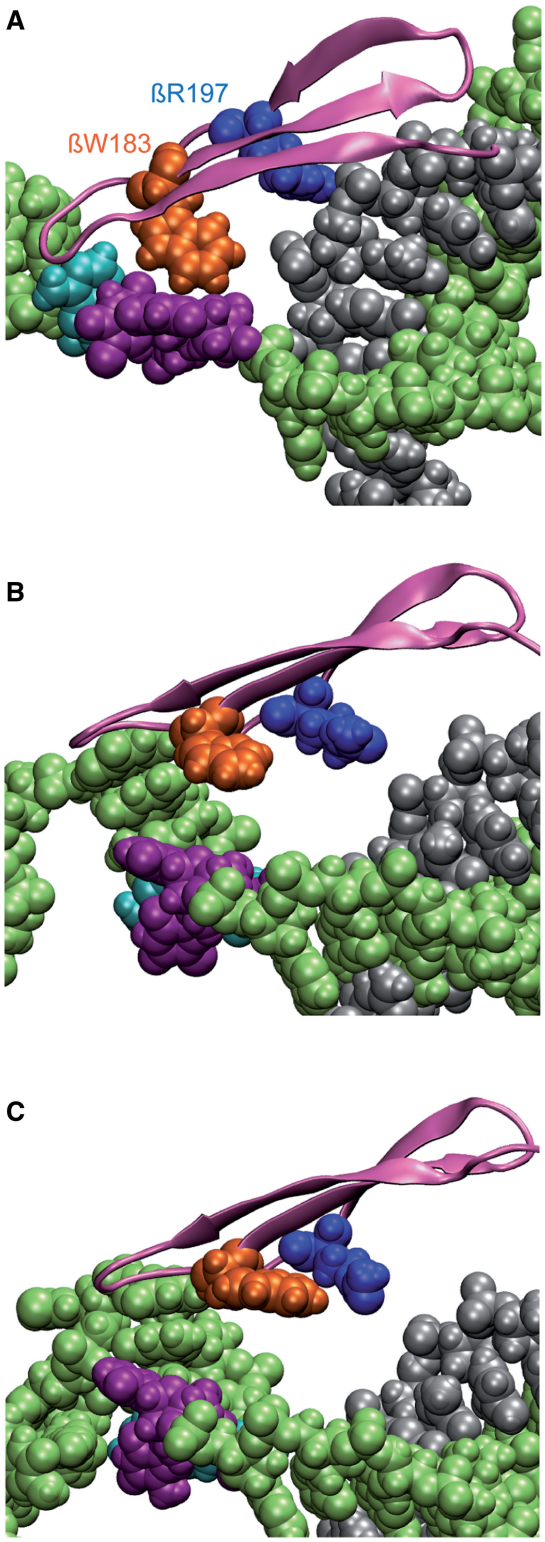

Figure 6. Molecular dynamics simulation of a TEC shows a cycle of engagement of βW183 (orange) with the non-template strand (green), followed by its dissociation and subsequent interaction with βR197 (blue). The template strand is shown in silver. (**A**) βW183 stably interacts with flipped out non-template strand bases (cyan and purple), βR197 interacts with the phosphodiester backbone of the template strand. (**B**) βW183 dissociates from the non-template strand. (**C**) βW183 engages with βR197 (also see Supplementary Movies S1 and S2).

by using promoter templates with a preopened +1 site, which partially rescued the transcription defects of switch region point mutations (32). No such recovery effect was observed with the βW183 variants, thus clearly arguing against a singular role in start site opening. Two of the mutants, βW183D and βW183R, displayed mildly suppressed phenotypes, whereas βW183A and βW183S performed WT-like on most of the templates (Figure 4). To exclude any sequence-specific bias on a start site opening role of W183, all four bases were tested in the non-template +1 site, but only the non-template +1G in combination with a template +1T resulted in a gain-of-function phenotype for βW183A and βW183S. Although this may suggest a sequence-specific requirement for the non-template strand +1 site, the uncertainties caused by the additional changes that were required to maintain the mismatch do not allow this effect to be unambiguously attributed to the non-template strand +1/W183 interaction. We therefore conclude that no strong evidence exists for βW183 to actively support start site opening as its sole function.

The aMD studies of βW183 in a transcription elongation complex, on the other hand, revealed that βW183 may undergo a cycle of making and breaking interactions with flipped out bases of the non-template strand (state A) but can also engage with another conserved arginine (R197, state B) residue in the beta subunit, which alternatively interacts with the phosphodiester backbone in state A. By creating strong alternating reaction biases towards either state A or state B, these interactions may act in the fashion of a molecular toggle, which contributes to template translocation and/or DNA scrunching. A similar role has been proposed for a pocket formed by βR151, βI445, βD446, βR451, βL538 and βV547, which accommodates the non-template +2 site in the initiation complex (16). This pocket finds its structural counterpart in the eukaryotic RNAPII system (35) and may represent a generic mechanism that recurs during elongation to facilitate translocation (36). We propose that the interactions between βW183 and the +1 base of the DNA non-template strand act as a thermodynamic sink (Figure 7): In the RPc and RPi, base-pairing interactions between the template and non-template +1 site are thermodynamically stable (Figure 7A) but are disrupted on establishment of the interaction network within the active centre. The equilibrium shift allows the non-template +1 base to flip out (Figure 7B). To fully drive the reaction towards the RPo, the now accessible base interacts with βW183 via interactions, which are thermodynamically favored (Figure 7C). On reaching a thermodynamically stable state, interactions between other RNAP residues and the DNA must be broken to alter the thermodynamically stable state of the βW183/+1 site interaction and to result in its dissociation. βW183 subsequently interacts with R197 to release it from its interaction with the phosphodiester backbone. Once both interactions are broken, the template can slide forward to reach another stable state by βW183 interacting with another flipped out base further downstream (Supplementary Movie S3).

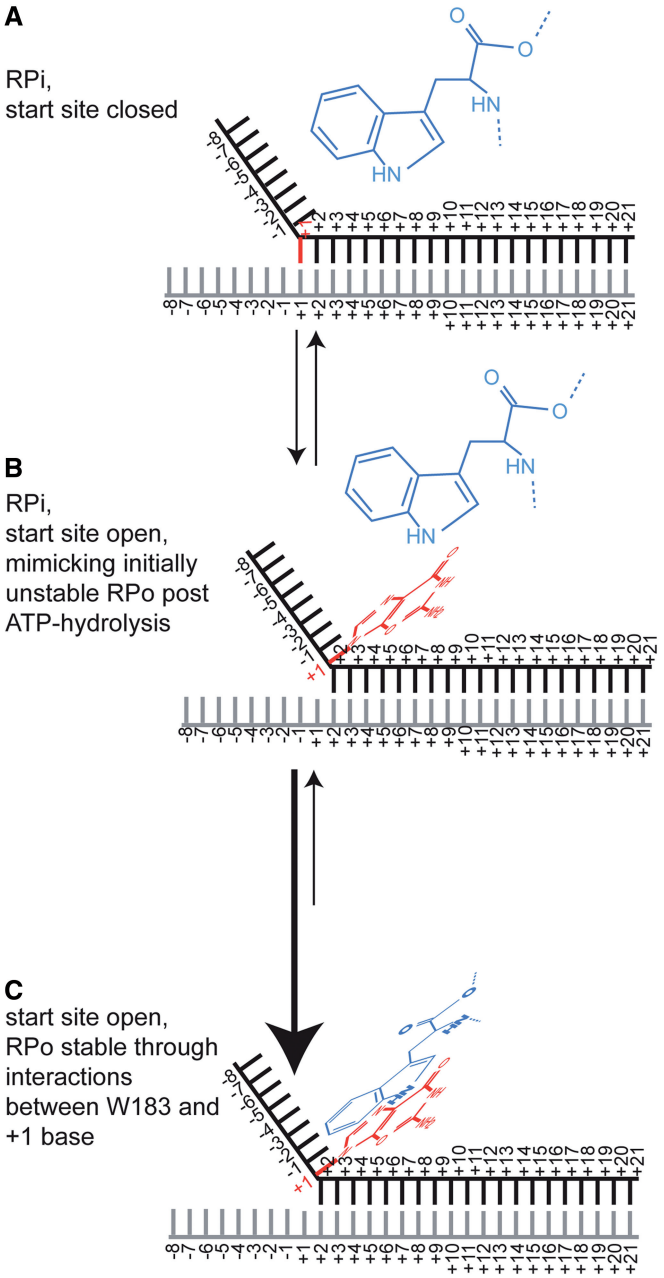

Figure 7. βW183/+1 site interactions act as a thermodynamic sink to stabilize the flipped out +1 site and drive RPo formation. (**A**) The start site is closed. (**B**) The switch regions trigger melting of the +1 site. (**C**) βW183 stabilizes the flipped out +1 site thus creating a thermodynamic bias towards a stable RPo (also see Supplementary Movie S3).

βW183 limits RPi activity and prevents the formation of bacterial nano-RNAs

The stabilization of abortive transcripts and their extension occurs on RPo formation (37). The bacterial enhancer-dependent transcription system allows us to capture and study the intermediate states (RPi) en route from the RPc to the RPo by trapping the complex prior to ATP hydrolysis (26,38). This reveals phenotypes that may escape studies performed in the σ^{70}-dependent transcription system where the RPi state is independent of activator binding and ATP hydrolysis (5) and thus cannot be readily trapped, stabilized and isolated for study. Performing trapping reactions for RPi formation with the βW183 mutants demonstrated that the amount of RPi formed was directly proportional to the amount of corresponding RPc, and that this proportion was constant across all the mutants and the WT (Figure 3). However, transcription activity reactions performed from such trapped complexes revealed strikingly superactive phenotypes of the mutants, most notably the βW183A and βW183S mutants (Figure 5C). Clearly, in the absence of the aromatic residue, constraints imposed on the RPi activity are lifted allowing extra transcription to occur prematurely. We observed a similar effect under ATP hydrolysis conditions with various non-template strand lengths (Figure 5D). The different lengths of the non-template strand might hinder the formation of the RNAP-non-template strand interactions that are required to progress into the open complex, and instead stall the complex in an RPi like state by mimicking different stages of DNA scrunching and/or promoter DNA engagement by RNAP (33,34). Burst and fast permanganate footprinting experiments showed that the RPo differs from the RPi by the position of the non-template strand in the active centre, allowing the assembly and DNA binding of the clamp and jaw domains (39). Transcription occurring in the RPi may limit the conversion to RPo by restricting necessary further conformational change in RNAP. Recent Förster resonance energy transfer analyses have demonstrated substantial flexibility of the transcription bubble in the active centre due to scrunching and unscrunching of the DNA template during the early stages of transcription initiation. Expansion and contraction of the transcription bubble promote the utilization of alternative upstream or downstream start sites (40). It seems plausible that variability in start site selection may result in the production of alternative transcripts. We argue that βW183 may be the key in preventing the formation of such alternative transcripts by limiting the transcriptional activity of the RPi during the various stages of DNA scrunching. Also, biasing towards RPi-dependent transcription by providing promoters with variable non-template strand lengths allowed the βW183 mutants to produce a larger number of short abortive RNAs in RPi (Figure 5C), which—along with intermediates of RNA degradation (41,42), products of RNA cleavage during elongation (43,44) and products of cyclic dinculeotide degradation (45–48) are one source of bacterial nano-RNAs (49–51). Such transcripts with a length of 2 to ~5 nt can significantly alter the intracellular gene expression profile by (i) competing with nucleotides as primers for transcription initiations and extending the 5′ end of the resulting transcripts; (ii) changing the position where transcription begins (52); and (iii) affecting the phosphorylation state—and accordingly the stability of a transcript—by changing the 5′ end (48,53). We propose that under normal conditions, βW183 keeps RPi activity in check to prevent such sporadic and uncontrolled accumulation of bacterial nano-RNAs.

CONCLUSION

We have revealed two critical functions of residue βW183, (i) in limiting the transcription activity of the RPi and thus preventing the formation of potentially detrimental bacterial nano-RNAs or alternative transcripts and (ii) in acting in a thermodynamic sink mechanism that creates a strong reaction bias towards a fully formed RPo or towards a translocated TEC. The thermodynamic context that βW183 functions in is likely to play a key role in fuelling the formation and disruption of interactions in a complex matrix that in their entirety drive the transcription process.

SUPPLEMENTARY DATA

Supplementary Data are available at NAR Online: Supplementary Table 1, Supplementary Figures 1–3 and Supplementary Movies 1–3.

ACKNOWLEDGEMENTS

The authors thank R. Wigneshweraraj, N. Zhang and N. Joly for reagents and M. Jovanovic and C. Engl for helpful comments on the manuscript.

FUNDING

Biotechnology and Biological Sciences Research Council [BB/H012249/1 supporting SCW to M.B.]; Medical Research Council [G1100057 to R.O.J.W.]. Funding for open access charge: Imperial College London and Biotechnology and Biological Sciences Research Council.

Conflict of interest statement. None declared.

REFERENCES

1. Werner,F. (2008) Structural evolution of multisubunit RNA polymerases. *Trends Microbiol.*, **16**, 247–250.
2. Cramer,P. (2002) Multisubunit RNA polymerases. *Curr. Opin. Struct. Biol.*, **12**, 89–97.
3. Ho,M.X., Hudson,B.P., Das,K., Arnold,E. and Ebright,R.H. (2009) Structures of RNA polymerase-antibiotic complexes. *Curr. Opin. Struct. Biol.*, **19**, 715–723.
4. Buck,M., Bose,D., Burrows,P., Cannon,W., Joly,N., Pape,T., Rappas,M., Schumacher,J., Wigneshweraraj,S. and Zhang,X. (2006) A second paradigm for gene activation in bacteria. *Biochem. Soc. Trans.*, **34**, 1067–1071.
5. Buck,M., Gallegos,M.T., Studholme,D.J., Guo,Y. and Gralla,J.D. (2000) The bacterial enhancer-dependent sigma(54) (sigma(N)) transcription factor. *J. Bacteriol.*, **182**, 4129–4136.
6. Wigneshweraraj,S.R., Burrows,P.C., Bordes,P., Schumacher,J., Rappas,M., Finn,R.D., Cannon,W.V., Zhang,X. and Buck,M. (2005) The second paradigm for activation of transcription. *Prog. Nucleic. Acid Res. Mol. Biol.*, **79**, 339–369.
7. Burrows,P.C., Wiesler,S.C., Pan,Z., Buck,M. and Wigneshweraraj,S.R. (2012) Bacterial virulence gene expression contributed by the alternative sigma factor sigma54. In: Alain,A.M.Filloux (ed.), *In Bacterial Regulatory Networks*. Caister Academic Press, UK, pp. 27–58.
8. Bose,D., Pape,T., Burrows,P.C., Rappas,M., Wigneshweraraj,S.R., Buck,M. and Zhang,X. (2008) Organization of an activator-bound RNA polymerase holoenzyme. *Mol. Cell*, **32**, 337–346.
9. Joly,N., Burrows,P.C. and Buck,M. (2008) An intramolecular route for coupling ATPase activity in AAA+ proteins for transcription activation. *J. Biol. Chem.*, **283**, 13725–13735.
10. Joly,N., Zhang,N., Buck,M. and Zhang,X. (2012) Coupling AAA protein function to regulated gene expression. *Biochim. Biophys. Acta*, **1823**, 108–116.
11. Rappas,M., Schumacher,J., Beuron,F., Niwa,H., Bordes,P., Wigneshweraraj,S., Keetch,C.A., Robinson,C.V., Buck,M. and Zhang,X. (2005) Structural insights into the activity of enhancer-binding proteins. *Science*, **307**, 1972–1975.
12. Zhang,X., Chaney,M., Wigneshweraraj,S.R., Schumacher,J., Bordes,P., Cannon,W. and Buck,M. (2002) Mechanochemical ATPases and transcriptional activation. *Mol. Microbiol.*, **45**, 895–903.
13. Bose,D., Joly,N., Pape,T., Rappas,M., Schumacher,J., Buck,M. and Zhang,X. (2008) Dissecting the ATP hydrolysis pathway of bacterial enhancer-binding proteins. *Biochem. Soc. Trans.*, **36**, 83–88.
14. Naryshkin,N., Revyakin,A., Kim,Y., Mekler,V. and Ebright,R.H. (2000) Structural organization of the RNA polymerase-promoter open complex. *Cell*, **101**, 601–611.
15. Feklistov,A. and Darst,S.A. (2011) Structural basis for promoter-10 element recognition by the bacterial RNA polymerase sigma subunit. *Cell*, **147**, 1257–1269.
16. Zhang,Y., Feng,Y., Chatterjee,S., Tuske,S., Ho,M.X., Arnold,E. and Ebright,R.H. (2012) Structural basis of transcription initiation. *Science*, **338**, 1076–1080.
17. Cramer,P., Bushnell,D.A. and Kornberg,R.D. (2001) Structural basis of transcription: RNA polymerase II at 2.8 angstrom resolution. *Science*, **292**, 1863–1876.
18. Chakraborty,A., Wang,D., Ebright,Y.W., Korlann,Y., Kortkhonjia,E., Kim,T., Chowdhury,S., Wigneshweraraj,S., Irschik,H., Jansen,R. *et al.* (2012) Opening and closing of the bacterial RNA polymerase clamp. *Science*, **337**, 591–595.
19. Wiesler,S.C., Burrows,P.C. and Buck,M. (2012) A dual switch controls bacterial enhancer-dependent transcription. *Nucleic Acids Res.*, **40**, 10878–10892.
20. Jovanovic,M., Burrows,P.C., Bose,D., Camara,B., Wiesler,S., Weinzierl,R.O., Zhang,X., Wigneshweraraj,S. and Buck,M. (2011) An activity map of the Escherichia coli RNA polymerase bridge helix. *J. Biol. Chem.*, **286**, 14469–14479.
21. Opalka,N., Brown,J., Lane,W.J., Twist,K.A., Landick,R., Asturias,F.J. and Darst,S.A. (2010) Complete structural model of Escherichia coli RNA polymerase from a hybrid approach. *PLoS Biol.*, **8**, pii: e1000483.
22. Wigneshweraraj,S.R., Nechaev,S., Bordes,P., Jones,S., Cannon,W., Severinov,K. and Buck,M. (2003) Enhancer-dependent transcription by bacterial RNA polymerase: the beta subunit downstream lobe is used by sigma 54 during open promoter complex formation. *Methods Enzymol.*, **370**, 646–657.
23. Joly,N., Rappas,M., Wigneshweraraj,S.R., Zhang,X. and Buck,M. (2007) Coupling nucleotide hydrolysis to transcription activation performance in a bacterial enhancer binding protein. *Mol. Microbiol.*, **66**, 583–595.
24. Jovanovic,M., Burrows,P.C., Bose,D., Camara,B., Wiesler,S., Zhang,X., Wigneshweraraj,S., Weinzierl,R.O. and Buck,M. (2011) Activity map of the *Escherichia coli* RNA polymerase bridge helix. *J. Biol. Chem.*, **286**, 14469–14479.
25. Rozovskaya,T.A., Rechinsky,V.O., Bibilashvili,R.S., Karpeisky,M., Tarusova,N.B., Khomutov,R.M. and Dixon,H.B. (1984) The mechanism of pyrophosphorolysis of RNA by RNA polymerase. Endowment of RNA polymerase with artificial exonuclease activity. *Biochem. J.*, **224**, 645–650.
26. Burrows,P.C., Joly,N. and Buck,M. (2010) A prehydrolysis state of an AAA+ ATPase supports transcription activation of an enhancer-dependent RNA polymerase. *Proc. Natl Acad. Sci. USA*, **107**, 9376–9381.
27. Zhang,N., Joly,N., Burrows,P.C., Jovanovic,M., Wigneshweraraj,S.R. and Buck,M. (2009) The role of the conserved phenylalanine in the sigma54-interacting GAFTGA motif of bacterial enhancer binding proteins. *Nucleic Acids Res.*, **37**, 5981–5992.
28. Pierce,L.C., Salomon-Ferrer,R., Augusto,F.d.O.C., McCammon,J.A. and Walker,R.C. (2012) Routine access to

millisecond time scale events with accelerated molecular dynamics. *J. Chem. Theory Comput.*, **8**, 2997–3002.
29. Gotz,A.W., Williamson,M.J., Xu,D., Poole,D., Le Grand,S. and Walker,R.C. (2012) Routine Microsecond Molecular Dynamics Simulations with AMBER on GPUs. 1. Generalized Born. *J. Chem. Theory Comput.*, **8**, 1542–1555.
30. Humphrey,W., Dalke,A. and Schulten,K. (1996) VMD: visual molecular dynamics. *J. Mol. Graph*, **14**, 33–38, 27–38.
31. Mekler,V., Minakhin,L. and Severinov,K. (2011) A critical role of downstream RNA polymerase-promoter interactions in the formation of initiation complex. *J. Biol. Chem.*, **286**, 22600–22608.
32. Wiesler,S.C., Burrows,P.C. and Buck,M. (2012) A dual switch controls bacterial enhancer-dependent transcription. *Nucleic Acids Res.*, **40**, 10878–10892.
33. Kapanidis,A.N., Margeat,E., Ho,S.O., Kortkhonjia,E., Weiss,S. and Ebright,R.H. (2006) Initial transcription by RNA polymerase proceeds through a DNA-scrunching mechanism. *Science*, **314**, 1144–1147.
34. Revyakin,A., Liu,C., Ebright,R.H. and Strick,T.R. (2006) Abortive initiation and productive initiation by RNA polymerase involve DNA scrunching. *Science*, **314**, 1139–1143.
35. Cheung,A.C. and Cramer,P. (2011) Structural basis of RNA polymerase II backtracking, arrest and reactivation. *Nature*, **471**, 249–253.
36. Hein,P.P., Palangat,M. and Landick,R. (2011) RNA transcript 3′-proximal sequence affects translocation bias of RNA polymerase. *Biochemistry*, **50**, 7002–7014.
37. Bochkareva,A. and Zenkin,N. (2013) The sigma70 region 1.2 regulates promoter escape by unwinding DNA downstream of the transcription start site. *Nucleic Acids Res.*, Feb 20 (epub ahead of print).
38. Chaney,M., Grande,R., Wigneshweraraj,S.R., Cannon,W., Casaz,P., Gallegos,M.T., Schumacher,J., Jones,S., Elderkin,S., Dago,A.E. *et al.* (2001) Binding of transcriptional activators to sigma 54 in the presence of the transition state analog ADP-aluminum fluoride: insights into activator mechanochemical action. *Genes Dev.*, **15**, 2282–2294.
39. Gries,T.J., Kontur,W.S., Capp,M.W., Saecker,R.M. and Record,M.T. Jr (2010) One-step DNA melting in the RNA polymerase cleft opens the initiation bubble to form an unstable open complex. *Proc. Natl Acad. Sci. USA*, **107**, 10418–10423.
40. Robb,N.C., Cordes,T., Hwang,L.C., Gryte,K., Duchi,D., Craggs,T.D., Santoso,Y., Weiss,S., Ebright,R.H. and Kapanidis,A.N. (2013) The transcription bubble of the RNA polymerase-promoter open complex exhibits conformational heterogeneity and millisecond-scale dynamics: implications for transcription start-site selection. *J. Mol. Biol.*, **425**, 875–885.
41. Belasco,J.G. (2010) All things must pass: contrasts and commonalities in eukaryotic and bacterial mRNA decay. *Nat. Rev. Mol. Cell Biol.*, **11**, 467–478.
42. Condon,C. (2007) Maturation and degradation of RNA in bacteria. *Curr. Opin. Microbiol.*, **10**, 271–278.
43. Fish,R.N. and Kane,C.M. (2002) Promoting elongation with transcript cleavage stimulatory factors. *Biochim. Biophys. Acta*, **1577**, 287–307.
44. Landick,R. (2006) The regulatory roles and mechanism of transcriptional pausing. *Biochem. Soc. Trans.*, **34**, 1062–1066.
45. Romling,U. and Amikam,D. (2006) Cyclic di-GMP as a second messenger. *Curr. Opin. Microbiol.*, **9**, 218–228.
46. Hengge,R. (2009) Principles of c-di-GMP signalling in bacteria. *Nat. Rev. Microbiol.*, **7**, 263–273.
47. Schirmer,T. and Jenal,U. (2009) Structural and mechanistic determinants of c-di-GMP signalling. *Nat. Rev. Microbiol.*, **7**, 724–735.
48. Nickels,B.E. and Dove,S.L. (2011) NanoRNAs: a class of small RNAs that can prime transcription initiation in bacteria. *J. Mol. Biol.*, **412**, 772–781.
49. Hsu,L.M. (2002) Promoter clearance and escape in prokaryotes. *Biochim. Biophys. Acta*, **1577**, 191–207.
50. Hsu,L.M. (2009) Monitoring abortive initiation. *Methods*, **47**, 25–36.
51. Goldman,S.R., Ebright,R.H. and Nickels,B.E. (2009) Direct detection of abortive RNA transcripts *in vivo*. *Science*, **324**, 927–928.
52. Vvedenskaya,I.O., Sharp,J.S., Goldman,S.R., Kanabar,P.N., Livny,J., Dove,S.L. and Nickels,B.E. (2012) Growth phase-dependent control of transcription start site selection and gene expression by nanoRNAs. *Genes Dev.*, **26**, 1498–1507.
53. Goldman,S.R., Sharp,J.S., Vvedenskaya,I.O., Livny,J., Dove,S.L. and Nickels,B.E. (2011) NanoRNAs prime transcription initiation *in vivo*. *Mol. Cell*, **42**, 817–825.